PRAMANA
— journal of
physics

Vol. 61, No. 6
December 2003
pp. 1079–1088

The continuum shell-model neutron states of ^{209}Pb

RAMENDRA NATH MAJUMDAR
Physics Department, Vivekananda College, 269, Diamond Harbour Road, Kolkata 700 063, India
Email: ramen@hp2.saha.ernet.in
Address for correspondence: 30/41 Attapara Lane, P.O. Sinthee, Kolkata 700 050, India

MS received 13 November 2001; revised 12 June 2003; accepted 23 June 2003

Abstract. The neutron strength distributions of the three high-spin $1k_{17/2}$, $2h_{11/2}$ and $1j_{13/2}$ states of ^{209}Pb have been obtained within the formalism of the core-polarisation effect where the effect of interaction of the neutron shell-model states of ^{209}Pb with the collective vibrational states (originating also from the giant resonances) have been taken into consideration. The theoretical results have been discussed in the light of works on $1k_{17/2}$, $2h_{11/2}$ and $1j_{13/2}$ neutron orbitals of ^{209}Pb. The shell-model energies of the neutron states have been obtained by Skyrme–Hartree–Fock method.

Keywords. Shell-model states; spectroscopic factors; core-polarisation and giant resonances.

PACS Nos 27.80.+W; 21.10.Pc; 21.10.Jx; 21.60.Cs; 21.10.Re

1. Introduction

In recent years we have observed abundant experimental results to understand the shell-model strength distributions of the high-spin orbitals of ^{208}Pb from both the stripping and pick-up reaction on ^{208}Pb target nucleus [1]. The nature of the attenuation of the shell-model states provides with the idea of the interaction of an odd particle with the doubly even magic core nucleus ^{208}Pb. For the discrete low-lying excited states, the depletion of the shell-model strength can be explained by the interaction of the single nucleon with the quadrupole and octupole vibrations of ^{208}Pb [2]. The spreading or damping of the high-lying excited states can be explained if we include the interaction of the shell-model states with the collective vibrational states from giant resonances. The particle-vibration coupling model can be applied to understand the spreading pattern of the shell-model states lying in continuum region. The single-particle states are distributed over many excited regions such as low-lying, continuum and statistical regions. The strength functions or spectroscopic factors of the high-lying states in continuum region give us accurate information about the structure of the state under study. Here the strong core-polarisation effect dominates the fragmentation of the single-particle state. In the framework of the present model, we have optimised the energies of the neutron states to get corroboration with the experimental results as regards of the energies and spectroscopic factors of the unbound high-spin shell-model states of ^{209}Pb.

Recently these three high-spin neutron states have been studied within the framework of quasi-particle phonon coupling model [3]. In the present theoretical works we will deduce the nature of the shell-model strength functions of the three high-spin unbound $1k_{17/2}$, $2h_{11/2}$ and $1j_{13/2}$ neutron states of ^{209}Pb. The interaction of these three unbound states with the collective vibrational states has been examined within the framework of core-polarisation scheme [2]. Here we have obtained the shell-model energies of the neutron states by Skyrme–Hartree–Fock (SHF) method [4]. For SHF, the shell-model neutron states have been obtained within the framework of spherically symmetric HF scheme. To get realistic nuclear compressibility, we have used effective Skyrme force in HF scheme. The salient features of the calculation based on both the core-polarisation effect and SHF method have been discussed below [5–7]. The SHF programme has been applied here without pairing force in neutron states as pairing effect is negligibly small in the case of ^{209}Pb. Our present work deviates from earlier findings [2,5] as all the particle states and their corresponding weight factors have been calculated using SHF method. As the vibrational nucleus ^{209}Pb consists of a single neutron in different shell-model orbitals over the doubly magic ^{208}Pb core, the usual pairing effect within BCS formalism becomes negligibly small. So we have excluded pairing formalism in our SHF approach while investigating the structure of the unbound shell-model states of ^{209}Pb. For the sake of detailed presentation, we have depicted SHF procedure with the BCS approach in the following section.

The core-polarisation effect has been elaborately described in our earlier works [2]. In the present work, we have included high-lying collective vibrational states arising from giant resonances in our core-particle interaction model. The SHF method has been depicted in refs [6] and [7]. Only the salient features of both the models have been described below.

2. The particle-core coupling model and Skyrme–Hartree–Fock scheme

2.1 *The particle-core coupling model*

For small surface distortions about a spherical shape, the vibrating nucleus generates an equipotential surface whose potential can be written in terms of λ-mode vibrational amplitude $\alpha_{\lambda\mu}$ as [5],

$$V(r,\alpha_{\lambda\mu}) = V_0\left[\frac{r}{1+\sum_{\lambda\mu}\alpha_{\lambda\mu}Y_{\lambda\mu}(\theta\phi)}\right]. \tag{1}$$

Expanding by Taylor's theorem about r,

$$V(r,\alpha_{\lambda\mu}) = V_0(r) - r\frac{\mathrm{d}V_0}{\mathrm{d}r}\sum_{\lambda\mu}\alpha_{\lambda\mu}Y_{\lambda\mu}(\theta,\phi)+\cdots. \tag{2}$$

Here $V_0(r)$ is the average one-body potential and $\alpha_{\lambda\mu}$ the vibrational amplitude. The leading order particle-vibrational term is linear in the amplitude $\alpha_{\lambda\mu}$. In a spherical nucleus ^{208}Pb, the coupling is the scalar product of the tensors $\alpha_{\lambda\mu}$ and $Y_{\lambda\mu}$ for the shape vibrations and this is,

$$H_{\text{int}} = K(r)(2\lambda+1)^{1/2}(\alpha_\lambda Y_\lambda(p))_0. \tag{3}$$

Here p in Y_λ takes care of a particle state that interacts with the collective vibrational state specified by α_λ.

$$K(r) = -r\frac{\mathrm{d}V_0}{\mathrm{d}r}. \tag{4}$$

V_0 is the single-particle potential in which the extra nucleon moves. The matrix elements of $K(r)$ has been kept fixed at 50 MeV and this has been discussed in the following section.

The shell-model neutron state $|j_2\rangle$ has been coupled with the vibrational $|\lambda^\pi\rangle$ spin state. Here λ indicates the angular momentum of the vibrational state of ^{208}Pb with parity π. In addition to the low-lying vibrational states, we have adopted high-lying vibrational states of the core nucleus ^{208}Pb arising from giant resonances in the core-particle coupling interaction scheme. These particular high-lying vibrational states have been differentiated by dash symbol over π, the parity of the vibrational states, that follow in the subsequent section. The diagonal terms of H are the sum of H_{vib} and H_{p} where $\langle H_{\mathrm{vib}}\rangle$ and $\langle H_{\mathrm{p}}\rangle$ are the energies of the λ-mode vibrational and j_2 single-particle states. Here one phonon $|\lambda\rangle$ mode of vibration has been taken into consideration [2]. The matrix elements of interaction are

$$\begin{aligned}\langle n_\lambda = 1 : \lambda\, j_2, j_1|H_{\mathrm{int}}|n_\lambda = 0, 0\, j_1, j_1\rangle &= \langle j_2|K(r)|j_1\rangle\langle j_2||Y_\lambda||j_1\rangle \\ &\quad \times(2j_1+1)^{-1/2}\langle\alpha_\lambda\rangle.\end{aligned} \tag{5}$$

α_λ is the zero point amplitude for the λ-mode of collective vibrational state of ^{208}Pb. It is [5],

$$\langle\alpha_\lambda\rangle = \frac{4\pi G_\lambda^{1/2}}{Z(\lambda+3)} \tag{6}$$

where

$$G_\lambda = \frac{B(E\lambda)}{B(E\lambda)_{W.U.}}. \tag{7}$$

The $B(E\lambda)$ is known from experiment. $\langle Y_\lambda\rangle$ is the spherical harmonic term whose matrix elements have been evaluated between the single particle states j_1 and j_2. The matrix elements of H_{int} have been weighted with $U_{j_1}V_{j_1} + U_{j_2}V_{j_2}$, where U and V are non-occupational and occupational probabilities of the relevant shell-model orbitals designated by j_1 or j_2.

2.2 *The Skyrme–Hartree–Fock scheme*

The two-body version of the adopted Skyrme interaction can be written [6,7] as,

$$\begin{aligned}V_{12}(\vec{r}_1,\vec{r}_2) &= t_0(1+x_0P_\sigma)\delta(\vec{r}) + t_1(1+x_1P_\sigma)\delta(\vec{r})[\vec{k}^2+\vec{k}'^2] \\ &\quad + t_2(1+x_2P_\sigma)\vec{k}'\delta(\vec{r})\vec{k} + t_3\rho^\infty(\vec{R})\delta(\vec{r}),\end{aligned} \tag{8}$$

where $\vec{k}$ is the operator $(\nabla_1-\nabla_2)/2i$ acting on the right, $\vec{k}'$ is the operator $-(\nabla_1-\nabla_2)/2i$ acting on the left, P_σ is the spin exchange operator, $\vec{r}$ is the reference distance from the nucleus and $\vec{R}$ is the nuclear radius.

The HF energy can be written in terms of Hamiltonian energy density $\Re$ as

$$E = \langle H \rangle = \int \Re(\rho, \tau, \vec{J}) \mathrm{d}^3 r,$$
$$\rho(r) = \sum_{i=1}^{A} |\phi_i(\vec{r})|^2,$$
$$\tau(\vec{r}) = \sum_{i=1}^{A} |\vec{\nabla}\phi_i(\vec{r})|^2,$$
$$\vec{J}(\vec{r}) = i \sum_{i=1}^{A} \phi_i^*(\vec{\sigma} X \vec{\nabla})\phi_i, \tag{9}$$

where $\rho(r), \tau(r)$ and $\vec{J}(\vec{r})$ are the nuclear density, kinetic energy density and spin density terms. The minimisation of $\langle H \rangle$ leads to a set of differential equations. The non-locality of HF potential appears through an effective mass m^* as,

$$\left\{ -\vec{\nabla}\frac{\hbar^2}{2m^*}\vec{\nabla} + U_q(r) + W(r)(-i\vec{\nabla} X \vec{\sigma}) \right\}, \phi_i = e_i \phi_i. \tag{10}$$

$$\begin{aligned} U_q(r) = {} & t_0 \left[\left(1 + \tfrac{1}{2}x_0\right)\rho - \left(x_0 + \tfrac{1}{2}\right)\rho_q \right] \\ & + \tfrac{1}{4}\left[t_1\left(1 + \tfrac{1}{2}x_1\right) + t_2\left(1 + \tfrac{1}{2}x_2\right) \right]\tau \\ & + \tfrac{1}{4}\left[t_2\left(\tfrac{1}{2} + x_2\right) - t_2\left(\frac{1}{2 + x_1}\right) \right]\tau_q \\ & + \tfrac{1}{8}\left[3t_1\left(\tfrac{1}{2} + x_1\right) + t_2\left(\tfrac{1}{2} + x_2\right) \right]\nabla^2\rho_q \\ & - \tfrac{1}{8}\left[3t_1\left(1 + \tfrac{1}{2}x_1\right) - t_2\left(1 + \tfrac{1}{2}x_2\right) \right]\nabla^2\rho \\ & + \tfrac{1}{6}t_3\rho^\alpha\left[\left(1 + \tfrac{1}{2}x_3\right)\rho - (x_3 + \tfrac{1}{2})\rho_q \right] + \tfrac{1}{12}\alpha t_3 \rho^{\alpha - 1} \\ & \times \left[\left(1 + \tfrac{1}{2}x_3\right)\rho^2 - \left(x_3 + \tfrac{1}{2}\right)(\rho_n^2 + \rho_p^2) \right] - b_4(\nabla J + \nabla J_q) + U_\mathrm{C}, \end{aligned} \tag{11}$$

$$W_q(r) = b_4(\nabla\rho + \nabla\rho_q) + \tfrac{1}{8}(t_1 - t_2)J_q - \tfrac{1}{8}(x_1 t_1 + x_2 t_2)J. \tag{12}$$

U_C denotes the Coulomb contribution to the potential, $b_4 = W_0/2$, $\rho = \rho_p + \rho_n$, $\tau = \tau_p + \tau_n$ and $\nabla J = \nabla J_p + \nabla J_n$. The matrix elements of HF Hamiltonian are set up as a basis of the eigenfunctions of an axially symmetric oscillator. The Hamiltonian is diagonalised in each subspace with good quantum number Ω.

The density dependent zero-range pairing force is

$$V^\tau(\vec{r}_1, \sigma_1, \vec{r}_2, \sigma_2) = V_0^\tau \frac{1 - \sigma_1\sigma_2}{4}\delta(\vec{r}_1 - \vec{r}_2) f\left(\frac{\vec{r}_1 + \vec{r}_2}{2}\right). \tag{13}$$

Here τ denotes neutron or proton and $f(r)$ is a density dependent function.

$$f(\vec{r}) = 1 - \rho(\vec{r})/\rho_0, \tag{14}$$

where $V_0^n = -1100$ MeV $\cdot$ fm^{-3} and ρ_0 is the reference density.

The pairing matrix element of protons and neutrons can be stated as

$$V^{\tau}_{ii'jj'} = V^{\tau}_0 \int \mathrm{d}(\vec{r})\rho_i(\vec{r})\rho_j(\vec{r}) f(\vec{r}) \tag{15}$$

and

$$\rho_i(\vec{r}) = \sum_{\sigma} |\phi_i(\vec{r}\sigma)|^2. \tag{16}$$

Here pairing influence in the vicinity of the Fermi surface has been considered by the energy of pairing correlation, E_{p}. That is,

$$E^{\tau}_{\mathrm{p}} = \sum_{ij} f_i \sqrt{\omega_i(1-\omega_i)} V^{\tau}_{ii'jj'} f_j \sqrt{\omega_j(1-\omega_j)}. \tag{17}$$

f_i is the cutoff factor and is given by the equation

$$f_i = \left(1 + \exp\left(\frac{\varepsilon_i - \lambda - \Delta\varepsilon}{\mu}\right)\right)^{-1}, \tag{18}$$

where μ is the chemical potential and ε is the Fermi energy with $\Delta\varepsilon = 5$ MeV and $\mu = 0.5$ MeV. The pairing energy and occupation probabilities are

$$E^{\tau}_{\mathrm{p}} = -\frac{1}{2}\sum \frac{f_j^2 \Delta_j^{r^2}}{\sqrt{(\varepsilon_j - \lambda)^2 + f_j^2 \Delta_j^{\tau^2}}}. \tag{19}$$

$$\omega_i = \frac{1}{2}\left[1 - \frac{\varepsilon_j - \lambda}{\sqrt{(\varepsilon_j - \lambda)^2 + f_j^2 \Delta_j^{r^2}}}\right]. \tag{20}$$

The gap parameters Δ^{τ}_i are derived from the solution

$$\Delta^{\tau}_i = -\frac{1}{2}\sum V^{\tau}_{ii'jj'} \frac{f_j^2 \Delta_j^{\tau}}{\sqrt{(\varepsilon_i - \lambda)^2 + f_j^2 \Delta_j^{\tau^2}}}. \tag{21}$$

When pairing effect is included with the gap parameter Δ^{τ}_i, we have minimised the following expression:

$$\langle H \rangle - \sum_i \Delta^{\tau}_i U_i V_i. \tag{22}$$

The quantities U_i and V_i are varied under constraints.

$$U_i^2 + V_i^2 = 1, \quad \sum_i V_i^2 = N. \tag{23}$$

Here U_i and V_i are the usual non-occupation and occupation probabilities of the shell-model states.

The HF mean field localises the nucleus. This transforms the center-of-mass of the whole nucleus oscillating in the mean field. The constraint is that the total momentum of the actual nuclear ground-state should be zero. In this way center-of-mass correction has been inducted into our calculation.

3. Results

First of all we have calculated neutron shell-model energies of ^{208}Pb. We have used SHF effective interaction by following the method of Beiner *et al* [8] and Mukherjee and Majumdar [9] and the calculated results have been compared with the experimental findings [10,11]. We have taken SHF parameters as

$$t_0 = -2645.000, \quad t_1 = 410.0, \quad t_2 = -135.0, \quad t_3 = 15595, \quad x_0 = 0.09,$$
$$x_1 = 0, \quad x_2 = 0, \quad x_3 = 0.$$

The energies of the neutron states from SHF method along with experimental results have been shown in table 1. In order to frame the Hamiltonian matrices, we have taken the neutron particle states of ^{208}Pb core and these single-particle states interact with all the vibrational states including the ones arising from giant resonances. The Hamiltonian matrices for the $9/2^+$, $17/2^+$, $11/2^-$ and $13/2^-$ states have been diagonalised to get eigenvalues and eigenvectors for the respective neutron orbital. From the calculated eigenfunctions, the neutron strengths are deduced from $a_{0j_2}^2$ values. The energies of $17/2^+$, $13/2^-$ and $11/2^-$ states have been estimated with respect to the ground state energy of $9/2^+$ state. Here $a_{0j_2}^2$ is the spectroscopic factor or the single-particle strength function of the j_2 shell-model state. From the diagonalisation of the Hamiltonian matrix of j_2 state, we have obtained the squared amplitude of the zero phonon coupled state. This is our strength function that we want to study for the unbound states of ^{209}Pb.

We have coupled all the neutron states (table 1) with the 2_1^+, $2^{+'}$, 4^+, 6^+, 8^+, 3_1^-, $3^{-'}$, 5_1^-, 5_2^-, 7^- and $1^{-'}$ collective vibrational states of ^{208}Pb to generate the Hamiltonian matrices. $2^{+'}3^{-'}$ and $1^{-'}$ are the collective states of ^{208}Pb arising from the giant resonances. Energies, deduced from SHF method, have been taken as the energies of the particle states of ^{209}Pb. We have considered the neutron in the shell corresponding to $N > 126$ and lying in $2g_{9/2}$, $2g_{7/2}$, $3d_{5/2}$, $3d_{3/2}$, $4s_{1/2}$, $1i_{11/2}$, $1k_{17/2}$, $1j_{15/2}$ and $2h_{11/2}$ shell-model orbitals. The energies of the unbound $1k_{17/2}$, $2h_{11/2}$ and $1j_{13/2}$ orbitals have been estimated by the extrapolation method. We have calculated the difference of binding energies ΔE_n for the well-known $2g_{9/2}$, $1i_{11/2}$, $2g_{7/2}$ and $1j_{15/2}$ states for $Z = 82$, $N = 126$ and $Z = 114$, $N = 184$ nuclei. Then the average value of ΔE_n has been calculated. From the average value of ΔE_n and the energies of the $1k_{17/2}$, $2h_{11/2}$ and $1j_{13/2}$ states of the nucleus

Table 1. The shell-model energies (MeV) of the neutron states calculated from Skyrme–Hartree–Fock method. The numerical values within bracket indicate experimental estimates [7,8].

$2g_{9/2}$	$2g_{7/2}$	$3d_{5/2}$	$3d_{3/2}$	$4s_{1/2}$
−4.1403	−1.0656	−1.7157	−0.5994	0
$1j_{13/2}$	$1j_{15/2}$	$2h_{11/2}$	$1k_{17/2}$	$3f_{7/2}$
6.6485	−1.7074	3.3036	3.4036	4.3057
$3f_{5/2}$	$4p_{3/2}$	$4p_{1/2}$	$1i_{11/2}$	$1i_{13/2}$
5.0235	6.0000	0	−2.5376	−9.5924(−9.0)
$2f_{7/2}$	$1h_{9/2}$	$3p_{3/2}$	$2f_{5/2}$	$3p_{3/2}$
−11.8890(−9.7)	−11.9310(−10.8)	−9.2918(−8.3)	−9.1900(−7.9)	−8.3320(−7.4)

Table 2. The collective vibrational states of ^{208}Pb [2,5]. The dash over λ^{π} indicates vibrational states arising from the giant resonances.

λ^{π}	2_1^+	$2^{+'}$	4^+	6^+	8^+	3_1^+
E (MeV)	4.08	10.50	4.32	4.42	4.61	2.61
$< \alpha_{\lambda}$	0.025	0.037	0.024	0.015	0.010	0.040
λ^{π}	$3^{-'}$	5_1^+	5_2^+	7^-	$1^{-'}$	–
E (MeV)	17.50	3.20	3.71	4.04	13.60	–
$< \alpha_{\lambda}$	0.011	0.017	0.010	0.100	0.010	–

Table 3. The shell-model energies and the spectroscopic factors of the discrete states of ^{209}Pb. The energy is in MeV and the spectroscopic factor is $a^2_{0_{j_2}}$, the squared amplitude of the zero phonon coupled state. The numerical values within the bracket indicate experimental estimates [12].

nlj_2	Energy	Spectroscopic factor
$2g_{9/2}$	0.00(0.00)	0.8(0.89)
$1i_{11/2}$	0.854(0.7790)	0.81(0.72)
$2g_{7/2}$	2.6(2.491)	0.7(0.79)
$1j_{15/2}$	1.24(1.423)	0.7(0.62)
$1j_{15/2}$	3.77(3.02)	0.06(0.085)

$Z = 114$, $N = 184$, the corresponding energies of the above three unbound states have been estimated by extrapolation method. The energies and vibrational amplitudes $\langle\alpha_{\lambda}\rangle$ of the λ^{π} vibrational states have been adopted from our recent works on ^{207}Pb [5]. The values of these quantities are depicted in table 2. The matrix elements of the radial function $\langle K(r)\rangle$ between shell-model neutron states have been calculated using harmonic oscillator wave functions of the relevant shell-model states with $\hbar\omega = 41A^{-1/3}$ MeV. This value has been kept fixed at 50 MeV and we have maintained this value in our earlier works on shell-model states of ^{208}Pb. The Hamiltonian matrices for the $9/2^+$, $5/2^+$, $7/2^+$, $15/2^-$, $17/2^+$, $13/2^-$, $17/2^+$ and $11/2^-$ states have been diagonalised to get eigenvalues and eigenfunctions. The results are shown in tables 3 and 4. The coincidence of the theoretical estimates with the experimental ones [12], as shown in table 3, proves the fidelity of the present model. The listed shell-model energies of the three unbound states along with their strength functions have been compared with the recent work [3] and table 4 shows the calculated results. Also the present core-polarisation is also successful in examining the behaviour of the unbound $i_{11/2}$ and $j_{13/2}$ states of ^{209}Bi as well [13]. The optimised parameters look convincing as the deduced energies of the shell-model states coincide with experiments [10,11] (table 1).

The distribution of these three high-spin states (table 4) show that the single-particle strengths are distributed over a large number of door-way collective configurations. The spreading pattern of the shell-model strengths shows the signature of the strong interaction of the shell-model state with the collective degrees of freedom, arising from both low and high energetic collective vibrational states of ^{208}Pb. The damping patterns of the $1k_{17/2}$, $2h_{11/2}$ and $1j_{13/2}$ neutron states corroborate with the experimental observations [3]. We observe from the results [3] that burden of the shell-model strengths of the three unbound shell-model $k_{17/2}$, $h_{11/2}$ and $j_{13/2}$ states centre at 8, 7 and 9.5 MeV excitation energies. Our results indicate that 8.2, 10 and 9.78 MeV states carry the burden of the neutron strengths of the specified three unbound orbital of ^{209}Pb. Moreover the usual damping pattern, as distinctly exhibited (p. 735 of ref. [3]), through see-saw nature of the cross-sections, corroborates with the theoretical estimates because we observe many weak fragments of these three states (table 4). The intrusion of the very high-spin states within 10 MeV excitation energy is unlikely because unperturbed energies of the shell-model states of very high-spin value (table 3) will lie much below 10 MeV. The fragments of these states having appreciable neutron strength will not scan the energy region (0–10 MeV) in as much as the strong perturbation that will result because of mixing with high lying collective states from the giant resonances. So we can exclude the presence of high-spin unbound orbitals except $k_{17/2}$, $h_{11/2}$ and $j_{13/2}$ within 10 MeV excitation energy of ^{209}Pb. The variation

Table 4. The spectroscopic factors of the three unbound neutron states of ^{209}Pb. E denotes excitation energy of the shell-model state in MeV and S is the spectroscopic factor. The experimental location of the three continuum states is within 6–10 MeV excitation energies [3].

$1j_{13/2}$ state		$2h_{11/2}$ state		$1k_{17/2}$ state	
E	S	E	S	E	S
5.00	0.005	4.5	0.30	4.4	0.02
5.444	0.018	5.2	0.016	5.0	0.30
5.9	0.012	5.6	0.020	5.2	0.03
6.5	0.010	5.85	0.03	5.4	0.080
9.78	0.5	10.005	0.54	5.8	0.020
10.1	0.44	10.8	0.38	8.2	0.500
10.56	0.25	11.1	0.16	9.12	0.12
11.0	0.33	11.8	0.12	9.9	0.16
12.5	0.18			10.0	0.17
				11.6	0.34
				12.5	0.44

Table 5. The spectroscopic factors of the three unbound neutron states of ^{209}Pb. E denotes excitation energy of the shell-model state in MeV and S is the spectroscopic factor. The numerical figures have been estimated without the inclusion of the high-lying collective states from giant resonances in setting up the Hamiltonian matrices.

$1j_{13/2}$ state		$2h_{11/2}$ state		$1k_{17/2}$ state	
E	S	E	S	E	S
3.40	0.105	3.8	0.10	3.6	0.12
4.50	0.118	4.0	0.068	3.86	0.15
5.5	0.412	4.6	0.320	4.8	0.08
5.8	0.040	5.80	0.63	5.6	0.68
6.70	0.86			5.8	0.120
				8.2	0.15

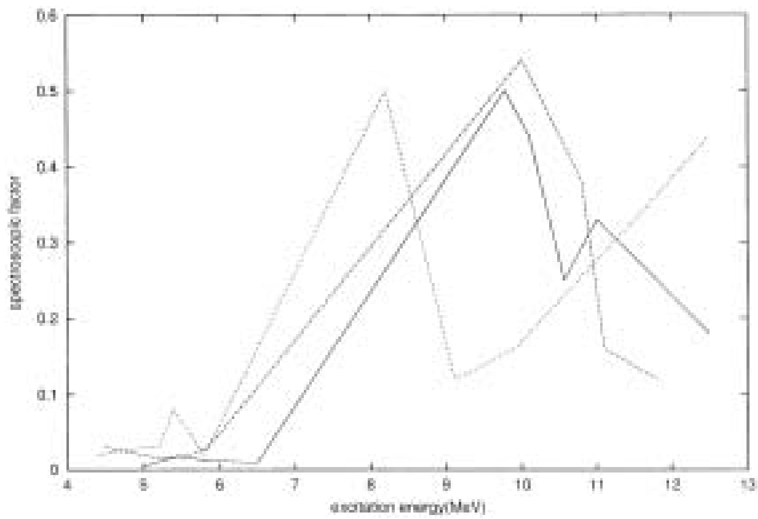

Figure 1. The distribution of the $1j_{13/2}$, $2h_{11/2}$ and $1k_{17/2}$ states of ^{209}Pb. The dotted, dashed and the continuous curves indicate the distribution corresponding to $1k_{17/2}$, $1j_{13/2}$ and $2h_{11/2}$ states respectively. The scaling of the curves also is shown in the figure.

of the spectroscopic factors against the excitation energies of these three unbound states is shown in figure 1. The figure clearly demonstrates the see-saw nature of the single-particle strengths in continuum region that has been observed from both experimental and the previous theoretical results [3].

The *S*-matrix method [14] with the incorporation of the two-fold approach based on nucleon absorption and inelastic break-up for the excitation of the nucleon has been developed to understand the transfer probability and cross-section for the continuum shell-model states of ^{208}Pb. As far as we know this is the only theoretical approach to estimate the cross-section for excitation of the highly energetic unbound shell-model states of ^{209}Pb available in literature.

In order to point out the effect of core-polarisation, arising from the highly excited collective vibrational states, we have also diagonalised the Hamiltonian matrices without the inclusion of the collective states from giant resonances. The calculated results are shown in table 5. It is observed from table 5 that almost all the single-particle strengths are exhausted below 8 MeV excitation energy of ^{209}Pb. So the gross signature of the presence of the appreciable spectroscopic factors of the excited $17/2^+$, $11/2^-$ and $13/2^-$ states cannot be obtained below 7 MeV. Table 4 further indicates that appreciable shell-model strengths of the three unbound states might extend beyond 8 MeV excitation energy as summed spectroscopic factor of the three individual states approaches unity as we proceed towards higher excitation energies.

The results of the *S*-matrix method [14] show that the overlapping of neutron strengths are coming from $1l_{19/2}$ and $1m_{21/2}$ orbitals. The precise analysis regarding neutron strengths from quantitative point of view lacks in this theoretical approach [14].

In conclusion, we observe that beyond 5 MeV excitation energy of ^{209}Pb, a certain part of the shell-model strength of the continuum states of ^{209}Pb can be identified to be of

$1k_{17/2}$, $2h_{11/2}$ and $1j_{13/2}$ origin. A clean spreading pattern of these two high-spin states can be understood from our theoretical approach. Also the present calculations show that the trend of the attenuation of the neutron strengths for these three neutron orbitals, that follow the experimental trend of the $2h_{11/2}$, $1j_{13/2}$ and $1k_{!7/2}$ states, is in sharp contrast with the other theoretical calculations based on *S*-matrix model scheme. The real loss of shell-model identities of these three unbound states can solely be understood based on core-particle coupling model interaction with the incorporation of collective vibrational states originating from the giant resonances of the doubly magic nucleus ^{208}Pb.

Acknowledgement

The financial assistance from the Department of Science and Technology (DST), Government of India, through the grant SP/S2/K-10/96 is gratefully acknowledged.

References

[1] S Gales *et al*, *Phys. Rep.* **166**, 125 (1988)
[2] R Majumdar, *Phys. Rev.* **C47**, 178 (1993)
[3] N van Giai *et al*, *Phys. Rev.* **C53**, 730 (1996)
[4] J Bartel *et al*, *Nucl. Phys.* **A386**, 79 (1982)
[5] R Majumdar, *Prog. Theor. Phys.* **92**, 565 (1994)
[6] M J Giannoni *et al*, *Phys. Rev.* **C21**, 2076 (1980)
[7] Y Shen *et al*, *Z. Phys.* **A356**, 133 (1996)
[8] B Beiner *et al*, *Phys. Scr.* **A10**, 84 (1974)
[9] P Mukherjee and R Majumdar, *Nucl. Phys.* **A294**, 73 (1978)
[10] J M G Goniez *et al*, *Nucl. Phys.* **A451**, 125 (1992)
[11] H de Vries *et al*, *At. Data Nucl. Data Tables* **36**, 445 (1987)
[12] M C Marmex *et al*, *Phys. Rev.* **C37**, 1942 (1988)
[13] R Majumdar, *J. Phys.* **G13**, 357 (1987)
[14] A Bonacorso and D M Brink, *Phys. Rev.* **C44**, 1559 (1991)